International Journal of Chemical, Materials and Biomolecular Sciences
ISSN: 2415-6620
Vol:5, No:2, 2011

Influence of Taguchi Selected Parameters on Properties of $CuO-ZrO_2$ Nanoparticles Produced via Sol-gel Method

H. Abdizadeh and Y. Vahidshad

***Abstract*—**The present paper discusses the selection of process parameters for obtaining optimal nanocrystallites size in the $CuO-ZrO_2$ catalyst. There are some parameters changing the inorganic structure which have an influence on the role of hydrolysis and condensation reaction. A statistical design test method is implemented in order to optimize the experimental conditions of $CuO-ZrO_2$ nanoparticles preparation. This method is applied for the experiments and L16 orthogonal array standard. The crystallites size is considered as an index. This index will be used for the analysis in the condition where the parameters vary. The effect of pH, H_2O/ precursor molar ratio (R), time and temperature of calcination, chelating agent and alcohol volume are particularity investigated among all other parameters. In accordance with the results of Taguchi, it is found that temperature has the greatest impact on the particle size. The pH and H_2O/ precursor molar ratio have low influences as compared with temperature. The alcohol volume as well as the time has almost no effect as compared with all other parameters. Temperature also has an influence on the morphology and amorphous structure of zirconia. The optimal conditions are determined by using Taguchi method. The nanocatalyst is studied by DTA-TG, XRD, EDS, SEM and TEM. The results of this research indicate that it is possible to vary the structure, morphology and properties of the sol-gel by controlling the above-mentioned parameters.

***Keywords*—**$CuO-ZrO_2$ Nanoparticles, Sol-gel, Taguchi method.

I. Introduction

THE $CuO-ZrO_2$ nanoparticles are usually used for generation of hydrogen from methanol in fuel cell system. Finer precursor powders give rise to larger specific areas in catalyst which result in a high hydrogen production [1]. In addition, hydrogen is used in large quantities in the chemical industry [2]. Several methods have been developed to prepare $CuO-ZrO_2$ nanoparticles, such as sol-gel [3], precipitation [4], microemulsion [5], template method and so on [4]. One of these methods, the sol-gel procedure, is a promising method to synthesis nanometer-sized particles. Sol-gel method has been successfully employed to produce nanoparticles. The structure, morphology and size of $CuO-ZrO_2$ nanoparticles obtained by sol-gel method are under the influence of various parameters such as pH, temperature, reaction time, reagent concentrations, catalyst nature, concentration, H_2O/precursor molar ratio (R), chelating agent, aging temperature, time and drying. The advantages of using zirconia as a catalyst support is that it is a unique metal oxide which explicitly possesses special chemical properties such as: (i) interacting strongly with the active phase; (ii) possessing a high thermal stability and being more chemically inert than classical oxides; (iii) being the only metal oxide which may possess all four chemical properties: namely acidity, basicity, reducing ability and oxidizing ability [6]. The application of zirconia as a catalyst support is promising and has been employed in many industrial important reactions such as hydro processing, oxidation of alcohols and synthesis of methanol and higher alcohols [7-9]. There are three well-defined polymorphs of zirconia. The monoclinic phase is stable up to 1174˚C. It then transforms into the tetragonal phase, which is further changed into the cubic phase at 2370˚C. The cubic phase is stable up to the melting point (2680˚C) of zirconia [5].

The efficient analysis of the complex system using statistical experimental design [10] and the Taguchi method [6, 11] has been performed recently. The statistical experimental design can determine the effect of the factors on characterization properties and the optimal conditions of factors [12]. This conventional parametric design of experiment approach is time-consuming and requires enormous rate of resources. Moreover, this approach fails to capture the interaction terms of various Xs. Taguchi statistical design is a powerful tool to screen the significant Xs out of many ones by conducting a relatively less number of experiments [13]. It uses the table of orthogonal arrays and analysis of variance (ANOVA) as the tool of analysis. ANOVA can estimate the impacts of a factor on the feature properties and structure. Conventional statistical experiment design can determine the optimal conditions on the basis of the measured values of the characteristic properties, while Taguchi method can determine the experimental conditions having the variability as the optimum conditions [12]. In this work, focus is on the effect of pH, H_2O/precursor molar ratio (R), and time and temperature calcination, chelating agent and alcohol volume.

H. Abdizadeh, Associate Professor, School of Metallurgy and Materials Engineering, University of Tehran, Tehran, Iran, P.O. Box: 14395-553. (phone: +98-21-61114085; fax: +98-21-88006076; e-mail: abdizade@ut.ac.ir).

Y. Vahidshad. M.Sc., School of Metallurgy and Materials Engineering, University of Tehran, Tehran, Iran. (e-mail: yvahidshad@yahoo.com)

II. Experimental Procedure

A. Synthesis

Samples of CuO-stabilized zirconia have been prepared employing the sol–gel technique. In a typical synthesis, 4.7g of zirconium isopropoxide (70wt. % solution in 1-propanol, Aldrich) has been dissolved in 40ml of dry isopropanol. To this solution, a specific amount of $Cu(NO_3)_2.3H_2O$ (99.9% Merck), has been dissolved in 10ml of isopropanol. Thi solution has been added under constant stirring to obtain clear and homogeneous solution. In this work, the ratio of Cu/Zr is fixed at 30/70 molar. Citric acid and acetic acid have been used in the solution before adding water and catalyst agent. Citric acid or acetic acid has been employed as a chelating agent. Then, a stoichiometric quantity of water has been used as a starting hydrolysis. The ratios of H_2O/precursor (R) and alcohol volume have been varied in the range of 0.18 to 1.5 and 33 to 77, respectively. Nitric acid or ammonia has been employed as a catalyst agent in order to regulate the pH. Depending on the pH, Nitric acid or ammonia is mixed in 10ml of isopropanol and introduced to the above solution to hydrolyze the zirconium isopropoxide. The solution pH has been selected between 2-4, 4-6, 6-8 and 8-10 in hydrolysis and condensation step. The obtained mixtures have been further stirred for 30 min and then 4 hr aged at 80˚C for drying until a thick transparent gel being formed. The resulting solid gel has been ground to a fine powder and subsequently heat-treated at different temperatures to study the structure, morphology and phase transformations. The samples have been heated for 3.5 and 5 hours at 400, 500, 600, and 700˚C (10˚C per minute). All of samples synthesis is according to Table 1. Cu–samples with a nominal Cu content of 30 mol % are prepared. The catalyst has been studied by DTA-TG, XRD, EDS, SEM and TEM.

B. Experimental Parameters

Taguchi's orthogonal array is chosen with six parameters that could affect the particle size (Table 1). The used orthogonal array of L-16 type is represented in Table 2. L and subscript 16 is denoting Latin square and the number of experiment, respectively. In addition, six column of the orthogonal array are assigned for alchol volume, temperature of calcination, time of calcination, pH, H_2O/precursor molar ratio and chelating agent. In this article, the results were analyzed statistically by the analysis of variance (ANOVA) method using Qualitek-4 software.

Table II
The Used Orthogonal Array of L-16 Type

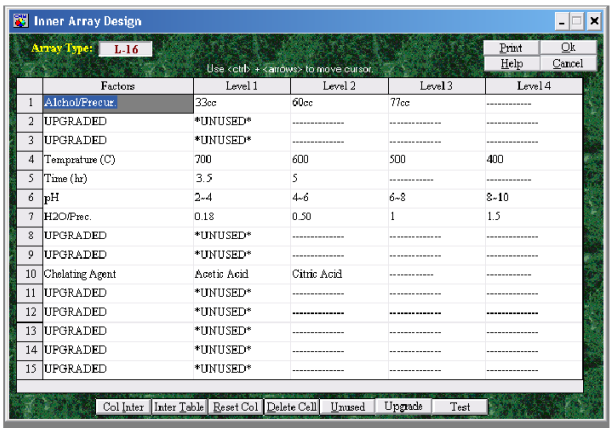

III. Results and Discussion

A. Taguchi array design and analysis of variance

The Taguchi orthogonal array design is used to identify the optimal conditions and to select the parameters having the most principal influence on the particle size. Table 3 shows the structure of Taguchi's orthogonal array design and its measurement results. The variance of the crystallites size of Table 3 is calculated, and the results are shown in Table 4 (standard method in Taguchi approach).

The purpose of the analysis of variance (ANOVA) is to investigate the factors which significantly affect the quality of characterization.

Table I
Parameters and Levels Used in This Experiment

	Factor	Levels			
		(1)	(2)	(3)	(4)
A	alcohol volume (cc)	33	60	77	
B	temperature of calcination (˚C)	700	600	500	400
C	time of calcination (hr)	3.5	5		
D	pH	2-4	4-6	6-8	8-10
E	R (H_2O/ precursor molar ratio) (cc)	0.18	0.5	1	1.5
F	chelating agent	Acetic acid	Citric acid		

In Table 4, S and V represent the sum of square of each column and the mean square of factor respectively. The influence of factors on catalyst synthesis can be estimated by the result of the ANOVA process. The F values are used to determine whether or not a control factor can be pooled (sum

of Squares Pooled) to an error term or not [14]. After estimating the values in the analysis of error variance, the value of FB is 6.156. However, the calcinations temperature is the only parameter that can have an impact on the crystallites size as compared with the other parameters.

The optimal conditions show the description and the expected performance at the optimum conditions. It is a common practice to include only the significant factors in the description.

TABLE III
EXPERIMENTAL MEASURED VALUES FOR PARTICLE SIZE OF CuO/ZrO_2 PARTICLE

Exp. No.	*Sample No.*	*A*	*B*	*C*	*D*	*E*	*F*	*Crystallite Size*		
								ZrO_2 (nm)	*CuO (nm)*	*Average Crystallite Size*
1	CZ-SG-13	***1***	***1***	***1***	***1***	***1***	***1***	22	20	21
2	CZ-SG-14	***1***	***2***	***1***	***2***	***2***	***2***	23	21	22
3	CZ-SG-8	***1***	***3***	***2***	***3***	***3***	***1***	13	12.2	12.6
4	CZ-SG-18	***1***	***4***	***2***	***4***	***4***	***2***	16.8	13.1	14.95
5	CZ-SG-15	***2***	***1***	***1***	***4***	***3***	***2***	19.3	17.2	18.25
6	CZ-SG-10	***2***	***2***	***1***	***3***	***4***	***1***	15.2	13.3	14.25
7	CZ-SG-19	***2***	***3***	***2***	***2***	***1***	***2***	13	12.8	12.9
8	CZ-SG-6	***2***	***4***	***2***	***1***	***2***	***1***	* ≈ 8	* ≈ 8	8
9	CZ-SG-7	***3***	***1***	***2***	***2***	***4***	***1***	21.3	19.6	20.45
10	CZ-SG-21	***3***	***2***	***2***	***1***	***3***	***2***	16	13.6	14.8
11	CZ-SG-11	***3***	***3***	***1***	***4***	***2***	***1***	10.3	9.7	10
12	CZ-SG-16	***3***	***4***	***1***	***3***	***1***	***2***	* ≈ 9	* ≈ 9	9
13	CZ-SG-20	***1***	***1***	***2***	***3***	***2***	***2***	22.5	19.7	21.1
14	CZ-SG-9	***1***	***2***	***2***	***4***	***1***	***1***	17	15	16
15	CZ-SG-17	***1***	***3***	***1***	***1***	***4***	***2***	10	9.5	9.75
16	CZ-SG-12	***1***	***4***	***1***	***2***	***3***	***1***	* ≈ 8.5	* ≈ 8.5	8.5

*Crystallite size measured by TEM, because samples are approximate

TABLE IV
THE ANOVA TABLE OF PARTICLE SIZE FOR THE UNPOOL METHOD

Factor	Sum of square (S)	DOF (f)	Variance (V)	F-Ratio (F)	Pure Sum (S)	Percent P (%)
A	20.906	2	10.453	0.72	0	0
B	267.926	3	89.308	6.156	224.409	63.85
C	4.049	1	4.049	0.279	0	0
D	13.991	3	4.663	0.321	0	0
E	6.65	3	2.216	0.152	0	0
F	8.925	1	8.925	0.615	0	0
Error	29.011	2	14.505			36.15
Total	351.462	15				100 %

B. Determination of optimal condition using Taguchi method

The main observed parameters allow viewing the important impacts on the results. This is dependent on the parameter levels which have been selected for the analysis. The term "main effect" represents the trend of influence of an assigned factor to the column or an interaction for which the column may be reserved. The figures in the Table represent the average effects of the factors. The labeled column indicates the difference of the average effects and is an additional piece of information. The main effects in this experiment are shown in Table 5.

The contribution may numerically increase or decrease the effects; depending on the quality characteristics chosen for the analysis. This results show that the optimum conditions are A at level 2, B at level 4, C at level 1, D at level 1, E at level 3, and F at level 1. Table 6 identifies these factors for optimum conditions. At the calcination treatment, the temperature of 400˚C produces more amorphous structure than crystallite structure, and identifies 500˚C as transition temperature for synthesis of CuO/ZrO_2 catalyst. The optimal condition is A2B3C1D1E3F1. After synthesis of the CuO/ZrO_2 nanoparticles at the optimum condition, the TEM micrograph showed that the particle size is between 7 to 10 nm.

C. The role of parameters on the structural and morphology of products

The high temperature in aging step favors a fast hydrolysis reaction, which in turn leads to the formation of a large number of small nuclei. The low temperature followed by a long aging time would permit the occurrence of Ostwald ripening to further narrow the size distribution [15].

TABLE V
THE MAIN EFFECTS TABLE OF PARTICLE SIZE FOR THE UNPOOL METHOD (AVERAGE EFFECTS OF FACTORS)

	Factor	Level Description	Level	Contribution
A	Alcohol	33	2	- 1.247
B	Temperature	400	4	- 4.485
C	Time	3.5	1	- 0.504
D	pH	2-4	1	- 1.21
E	R (H_2O/ precursor molar ratio)	1	3	- 1.06
F	Chelating Agent	Acetic Acid	1	- 0.747
Total contribution from all factors				- 9.254
Current grand average of performance				14.596
Expected result at optimum condition				5.343

	Factor	Level 1	Level 2	Level 3	Level 4
A	Alcohol	15.737	13.35	13.562	
B	Temperature	20.2	16.672	11.312	10.112
C	Time	14.093	15.099		
D	pH	13.387	15.962	14.237	14.8
E	R (H_2O/ precursor molar ratio)	14.725	15.274	13.537	14.85
F	Chelating Agent	13.85	15.343		

At synthesized nanocatalyst from sol-gel method, for acid-catalyzed reaction, the first step of the hydrolysis is the fastest one, and the product of this step also undergoes the fastest condensation. Hence, an open network structure results initially, following by further hydrolysis and cross-condensation reaction. In a base-catalyzed reaction, the hydrolysis steps occur increasingly and rapidly, and the fully hydrolyzed species undergo the fastest condensation reaction. As a consequence, in base-catalyzed reactions, highly cross-linked large sol particles are initially obtained [16]. Condensation reaction under a basic condition yields three-dimensional structure instead of a linear structure which occurs under an acidic condition [15]. The most obvious effect of the increased value of (H_2O/precursor) molar ratio is the acceleration of the hydrolysis reaction. Additionally, higher values of (H_2O/precursor) molar ratio caused more complete hydrolysis of monomers before that significant condensation occurs [17].

Polymerization to form the bonds occurs by either an alcohol-producing or a water-producing condensation reaction. The condensation products are monomer, dimer, linear trimer, cyclic trimer, cyclic tetramer, and higher order rings. This sequence of condensation requires both depolymerization (ring opening) and the availability of monomers which are in solution equilibrium with the oligomeric species and/or are generated by depolymerization [17]. The rate of these ring opening polymerizations and monomer addition reactions depends on the environmental pH. Condensation preferentially occurs between more highly condensed species and those less highly condensed and somewhat neutral. This suggests that the rate of dimerization is low, however, once dimers form, they react preferentially with monomers to form trimers, which in turn react with monomers to form tetramers [16]. The chelating agent which produces the 3-D structure is another way to control the reactivity of the alkoxides. After drying, the gel is heated to initiate pyrolysis of the organic species, resulting in agglomerated submicron oxide particles [16].

D. Thermal analysis of CuO-ZrO_2 catalysts

As mentioned in part 2.2, the process of calcination of the dried xerogel is studied by thermal analysis (TG/DTA). The small dried xerogel samples are analyzed at a heating rate of 10˚C/min at air. The TG/DTA results are shown in Figure 1.

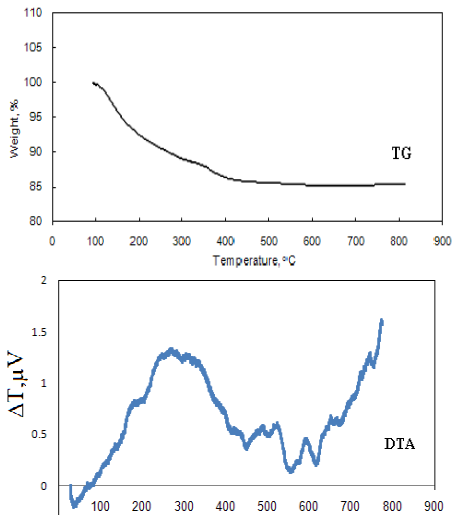

Fig. 1 Thermal analysis of the CuO/ZrO_2 nanoparticles

by TG-DTA simultaneous analysis. For the copper hydroxide and zirconium hydroxide, the total weight loss obtained after calcination up to 800˚C is about 14.0%. The DTA curve obtained for this hydroxide solid illustrates this modification.
For the $Cu(OH)_2$ /$Zr(OH)_4$ sample, an endothermic peak appeared at 300 to 450˚C. This peak indicates the exit of structural water, and also a change in the amorphous structure to cubic crystallite phase. At 500-550°C, an exothermic peak is appeared. The peak point indicates that some part of the cubic phase is transformed into the monoclinic phase. This is confirmed by XRD pattern (Figure 2). Furthermore, at 600˚C, an exothermic peak appeared. This peak indicates that part of monoclinic phase transforms to cubic (or tetragonal) phase, which is confirmed by XRD pattern.

E. XRD phase analysis of CuO-ZrO_2 catalysts

X-ray diffraction patterns are studied on a Philips analyzer using Ni filtered Co Kα (λ=1.78 Å) radiation. The structure changes of the zirconia-supported copper oxide catalysts investigated from samples synthesized at different conditions are shown in Figure 2. Zirconia exists in three well-established polymorphs: the monoclinic [JCPDS 37-1484, 13-0307, and 05-0543], tetragonal [JCPDS 17-0923, 14-0536, 02-0733], and cubic phases [JCPDS 03-0640, 07-0337, 27-0997]. The powder with the amorphous phase, $Cu(OH)_2$ and $Zr(OH)_4$ like structure, exist when the calcination temperature is beyond 500˚C. Yong Sheng Zhang et al. [16] have demonstrated that as the calcination temperature rose, the half maximum attenuated gradually, implying the growing of crystallites grain.

For samples CZ-SG-6, 12, 16 and 19 calcined at 400˚C, the $_2$ and CuO peaks are very weak. Furthermore, it is obvious that moving from sample 6 to 14, the intensity of the experience main peaks increases which indicates the growth and integrity of crystal particle. As the calcination temperature increases, the CuO/ZrO_2 crystallites peak become sharper and sharper; indicating the particle size of CuO/ZrO_2 became larger and larger. The average calculated crystallites size of CuO and ZrO_2, using Scherrer's equation, are listed in Table 7. The crystalline structure of zirconia used in the present study is found to be cubic and tetragonal phases as the predominant structures. The presence of cubic phase is detected in the Cu-stabilized zirconia, where the overlapping peaks of cubic and tetragonal zirconia can not be distinguished. Furthermore, the monoclinic phase can be seen with cubic and tetragonal phases at synthesized samples of CZ-SG-7, 15, and 20. Also, CuO (tenorite) exists at the related calcination temperature and time. This phenomenon indicates that there might be an interaction between the copper oxide and zirconium oxide particles. In fact, the phase remains stabilized even in a low temperature, resulting the cubic phase is produced. This is due to the interaction between Cu and Zr. Also, the results from Table 7 and Figure 2 indicate that the size changes of crystallites vary with the reaction conditions.

The XRD patterns of the xerogel are almost dependent on the aging temperature, pH, H2O/precursor and chelating agent. The particle size at samples CZ-SG-17, 11, 19, and 8 are the smallest sizes, and for the samples CZ-SG-14, 20, 13, and 7 are the largest sizes among all samples. This variation particle size is resulting from parameters described in subsection 3.3.

The breadths of the diffraction lines are usually described by the full width at half maximum (FWHM).

TABLE VII
PHYSICAL PROPERTIES OF CATALYSTS

Samples No.		2θ [˚] (ZrO_2)	2θ [˚] (CuO)	Crystallite size (XRD) (nm) d(ZrO_2)	Crystallite size (XRD) (nm) d(CuO)	XRD phase (ZrO_2)
1	CZ-SG-13	35.29	41.63	22	20	c-ZrO_2 + t-ZrO_2
2	CZ-SG-14	35.56	41.40	23	21	c-ZrO_2 + t-ZrO_2
3	CZ-SG-8	35.33	41.38	13	12.2	c-ZrO_2 + t-ZrO_2
4	CZ-SG-18	35.28	41.25	16.8	13.1	c-ZrO_2 + t-ZrO_2
5	CZ-SG-15	35.40	41.55	19.3	17.2	c-ZrO_2 + t-ZrO_2 + m-ZrO_2
6	CZ-SG-10	35.20	41.34	15.2	13.3	c-ZrO_2 + t-ZrO_2
7	CZ-SG-19	35.36	41.39	13	12.8	c-ZrO_2 + t-ZrO_2
8	CZ-SG-6	28.76	41.44	* ≈ 8	* ≈ 8	c-ZrO_2 + t-ZrO_2
9	CZ-SG-7	32.84	41.60	21.3	19.6	c-ZrO_2 + t-ZrO_2 + m-ZrO_2
10	CZ-SG-21	35.49	41.61	16	13.6	c-ZrO_2 + t-ZrO_2
11	CZ-SG-11	35.65	41.49	10.3	9.7	c-ZrO_2 + t-ZrO_2
12	CZ-SG-16	35.73	41.15	* ≈ 9	* ≈ 9	c-ZrO_2 + t-ZrO_2
13	CZ-SG-20	35.27	41.45	22.5	19.7	c-ZrO_2 + t-ZrO_2 + m-ZrO_2
14	CZ-SG-9	35.14	41.56	17	15	c-ZrO_2 + t-ZrO_2
15	CZ-SG-17	35.54	41.48	10	9.5	c-ZrO_2 + t-ZrO_2
16	CZ-SG-12	35.99	41.41	* ≈ 8.5	* ≈ 8.5	c-ZrO_2 + t-ZrO_2

ZrO

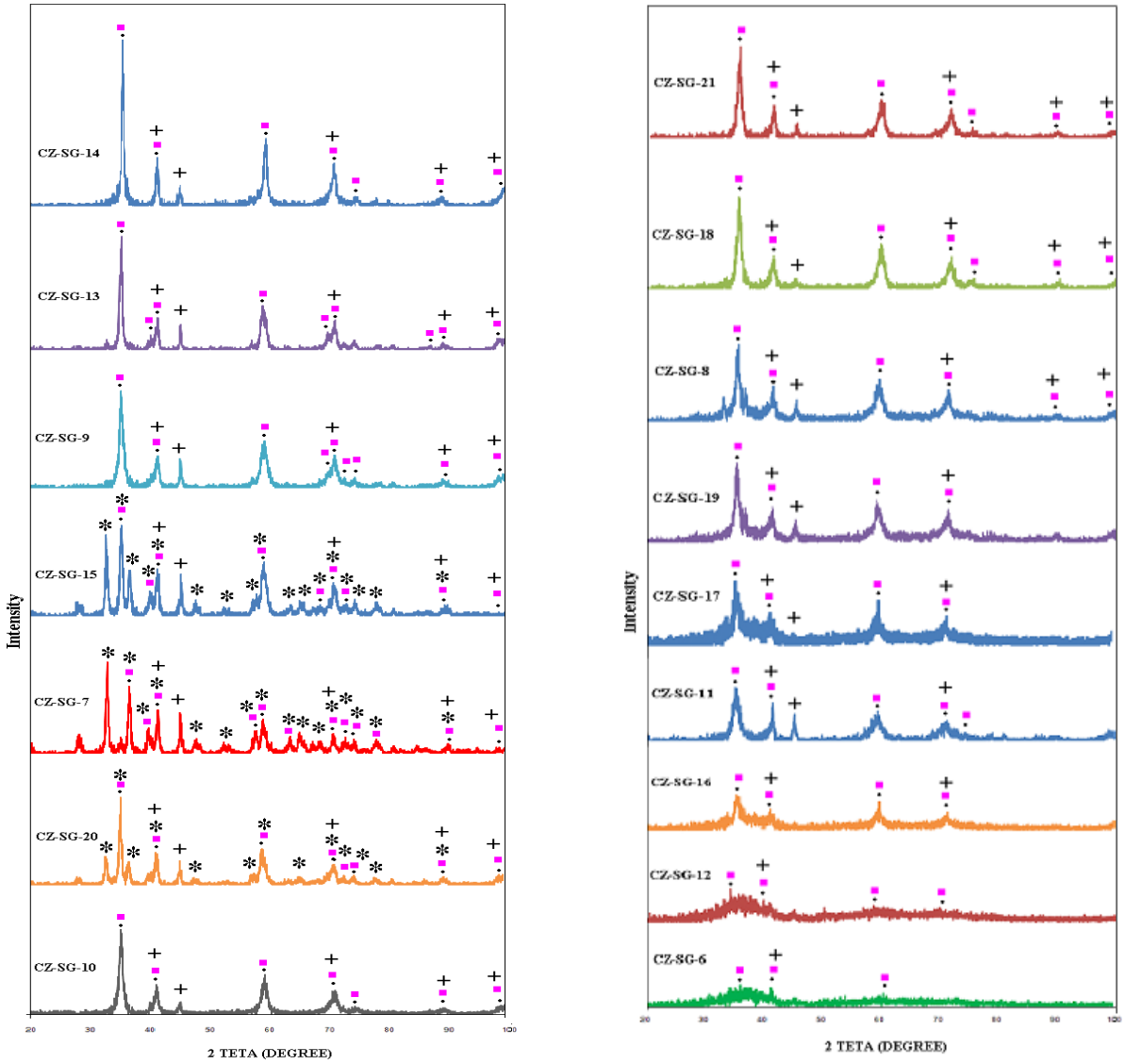

Fig. 2 XRD patterns of CuO-ZrO_2 nanoparticles: (+) CuO, (■) t-ZrO_2, (▪) c-ZrO_2, (*) m- ZrO_2

Regarding the intensity and the width of picks, these parameters can be defined easily from the diffraction lines. Line broadening occurs, when many small crystallites with fewer lattice planes are present in the powder. The estimation of the crystallites size could be realized by relating the peak width of a broadened Scherrer formula (Equation 1) [16].

$$\beta = \frac{\lambda * K}{L * \cos\theta} \quad (1)$$

Where, β=FWHM, λ=wavelength, K= form factor: 0.89 for cubic and 0.94 for spherical crystallites, L=crystallite thickness, θ= Bragg angle.

F. SEM and TEM photographs

Figure 3 shows the EDS spectrum of the particle of CZ-SG-14 sample that is specified by using (×) on Figure 6. As shown in Figure 2, both Cu and Zr are incorporated into nanoparticles structure.

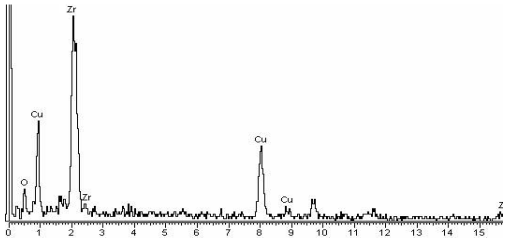

Fig. 3 EDX spectrum of CuO-ZrO2 nanoparticles

The specific surface area of catalyst decreases with the increase of a particle size at the calcination step [18]. The BET surface area of catalysts is in relation with particle size; with the rise of calcination temperature and time, the particle size agglomeration increased [16]. However, decreasing the crystallites size, the narrow distribution of particles and the lower particles agglomeration can realize a high specific surface area for the catalyst. As investigated in this work, the morphology of synthesized powders under the different conditions is observed in Figure 4. The morphology of synthesized particle with pH 4 to 8, exhibits more equiaxed microstructure and higher uniform particles (CZ-SG-19, 14, 16, and 20). The SEM picture illustrates that CZ-SG-19, CZ-SG-17, and CZ-SG-14 samples have the lowest agglomerated particles as compared with others. As the result of this research, when the calcination temperature increased beyond 500˚C up to 700˚C, the surface area decreased and at the same time, the pore size increased. This is due to metallic oxide particles shrinkage and agglomeration when they are calcined at high temperatures.

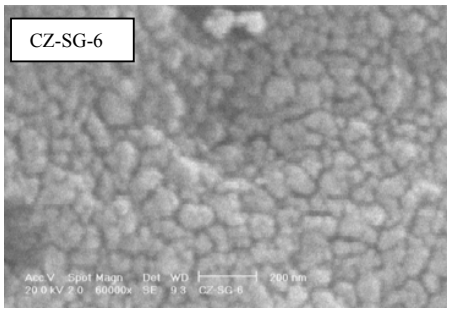

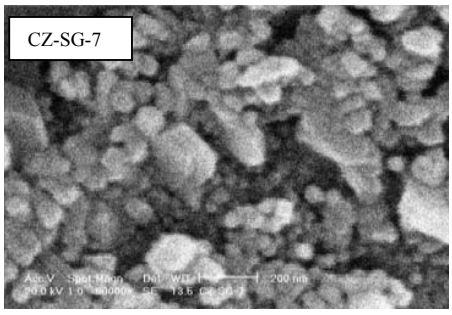

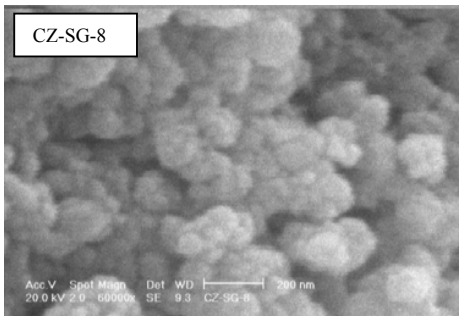

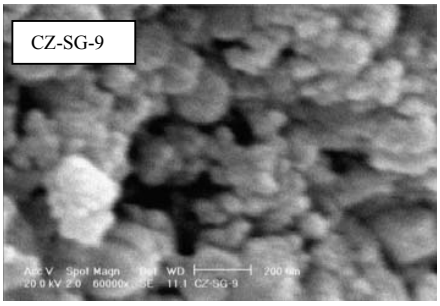

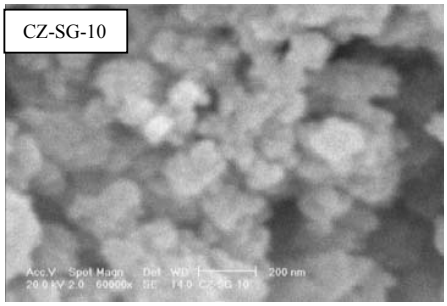

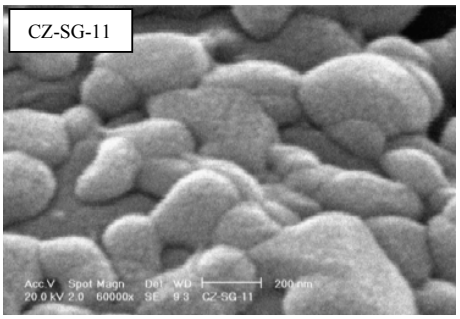

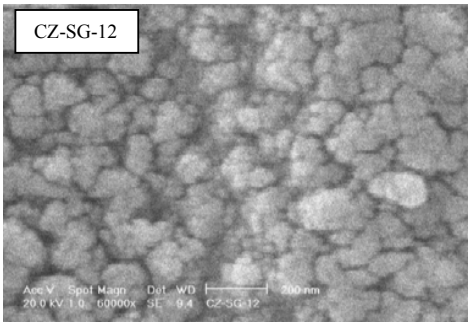

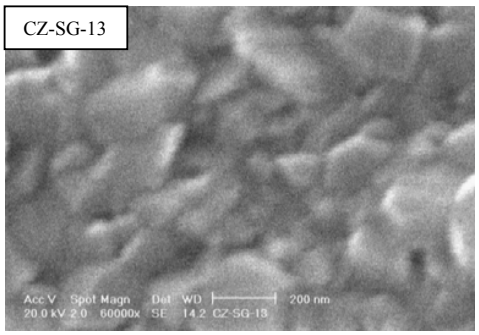

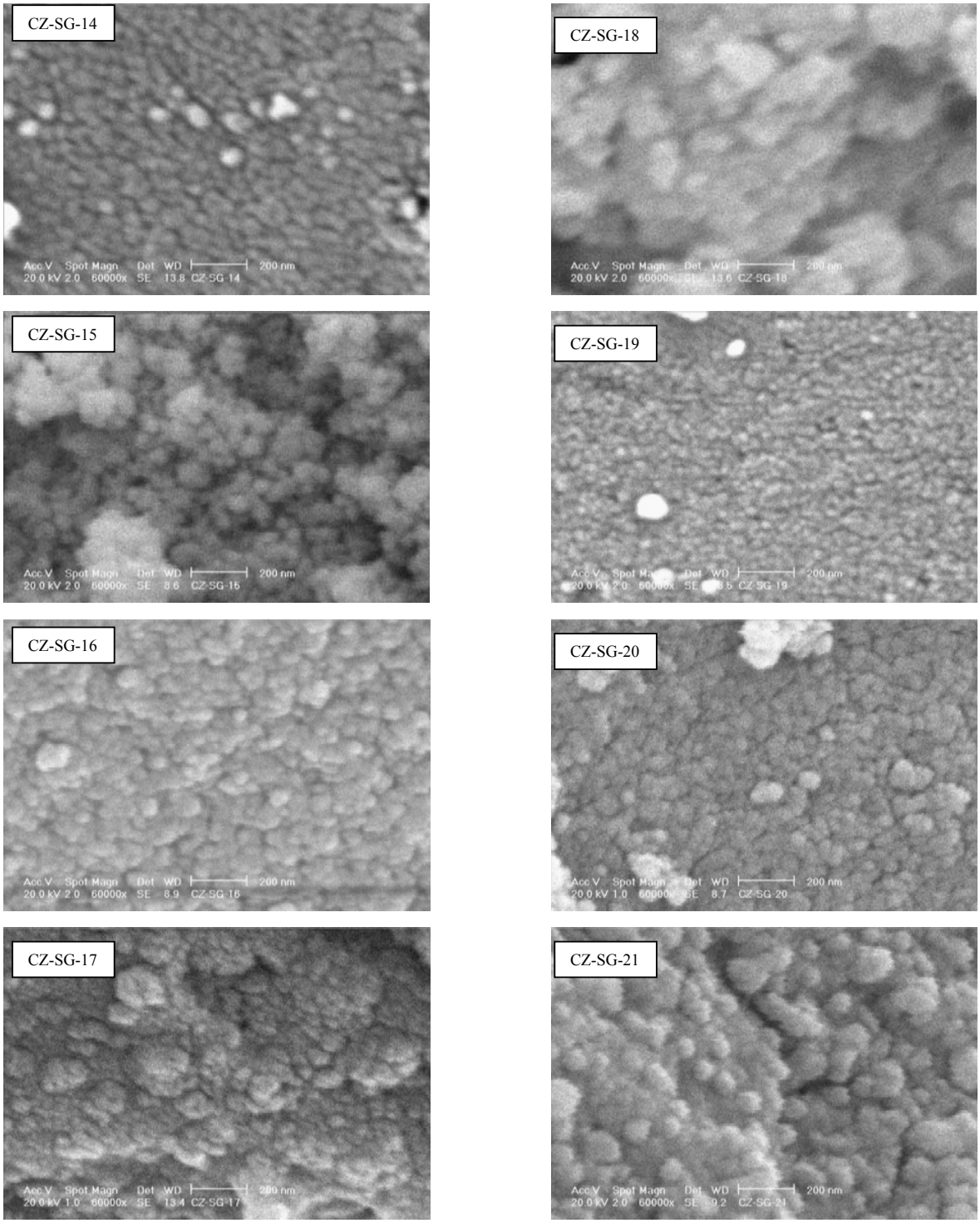

Fig. 4 SEM micrographs of nanoparticles synthesized in various conditions and parameters

Zeiss-EM10C (100kev) Transmission Electron Microscopy is used to examine the morphology of the samples. Figure 5 shows the photograph of the samples synthesized at optimized condition. The obtained nanoparticles have shown relatively uniform and rounded shapes with a narrow size distribution. According to the measurements performed on the TEM images, the particle size ranges from 9 to 14 nm for the sample which is synthesized in the optimal condition.

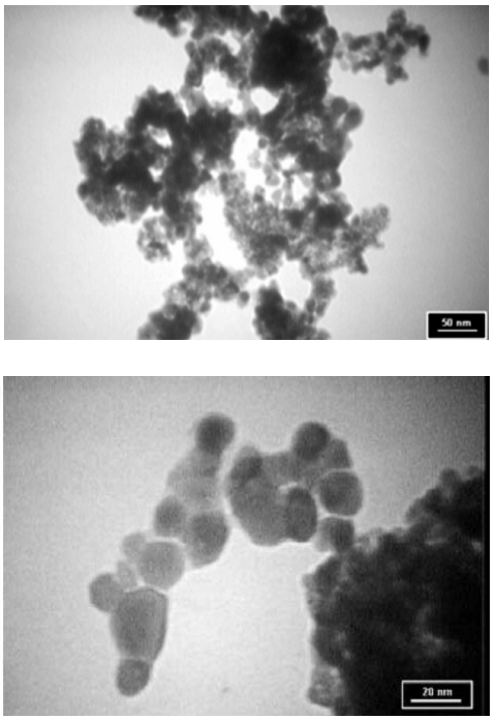

Fig. 5 TEM micrographs of CuO/ZrO_2

IV. CONCLUSIONS

The influence of the process parameters on the morphology and structure of nanoparticles produced with sol-gel method has been investigated. The study has led to the following conclusions:

- The XRD data indicate that cubic ZrO_2 and a lower amount of tetragonal ZrO_2 are obtained for the calcination temperatures from 500˚C up to 700˚C. The ZrO_2 stablization is subject to the interaction between Cu and Zr.
- An increase in calcination temperature results in the particle size increase.
- Samples synthesized at acidic and basic conditions result in decreasing of particle size as compared with the neutral pH.
- With molar relation of (H_2O/precursore)=4, the optimum hydrolysis and condensation rate is obtained, resulting in a smaller particle size among all samples.
- The use of an acetic acid as a chelating agent results in smaller particle size among all samples.
- The alcohol volume and calcination time have no influence on the particle size.
- The results indicate that the calcination temperature has the largest influence on the particle size among all parameters.

REFERENCES

[1] C. Cuciu, A.C. Hoffmann, and A.Vik, the effect of calcination and precursor proportion of YSZ nanoparticles obtained by modified sol- gel route, Department of Physics and Technology, University of Bergen Norway. Allegaten 55, Chemical Engineering Journal, **-***, (2007).
[2] M. Gradzielski, M. Lerch, and R. Schlögl, Microstructural Modifications of Copper Zinc Oxide Catalysts as a Function of Precipitate Ageing: university of Berlin, pp 3-6, (2003).
[3] M.K. Dongare, V. Ramaswamy, C.S. Gopinath, A.V. Ramaswamy, S. Scheurell, M. Brueckner, and E. Kemnitz, Oxidation activity and 18O-isotope exchange behavior of Cu-stabilized cubic zirconia, Journal of Catalysis 199, 209–216, (2001).
[4] I. Ritzkopf, S. Vukojevic, C. Weidenthaler, J.D. Grunwaldt, and F. Schuth, Decreased CO production in methanol steam reforming over Cu/ZrO2 catalysts prepared by the microemulsion technique, Applied Catalysis A: General 302, 215–223, (2006).
[5] V. Ramaswamy, M. Bhagwat, D. Srinivas, and A.V. Ramaswamy, 2004, Structural and spectral features of nano-crystalline copper-stabilized zirconia, Catalysis Today 97, 63–70.
[6] J.M. Liu, P.Y. Lu, and W.K. Weng, Studies on modifications of ITO surfaces in OLED devices by Taguchi methods, Materials Science and Engineering: B85, 209, (2001).
[7] W.J. Shen, Y. Ichihashi, and Y. Matsumura, Low temperature methanol synthesis from carbon monoxide and hydrogen over ceria supported copper catalyst, Applied Catalysis A: General 282, 221-226, (2005).
[8] S.H. Liu, G.K. Chuah, and S. Jaenicke, Liquid-phase Oppenauer oxidation of primary allylic and benzylic alcohols to corresponding aldehydes by solid zirconia catalysts, Juornal of Molecular Catalysis A: Chemical 220 Witco Chemical Company, 267-274, (2004).
[9] D. He, Y. Ding, H. Luo, and C. Li., Effects of zirconia phase on the synthesis of higher alcohols over zirconia and modified zirconia, Juornal of Molecular Catalysis A: Chemical 208, 267-271, (2004).
[10] R. D. Yang, R. R. Mater, and A. F. Fortheringham, Journal of material Science, 36, 3097, (2001).
[11] S.K. Park, K.D. Kim, and H.T. Kim, Applying the Taguchi method to the optimization for the synthesis of TiO2 nanoparticles by hydrolysis of TEOT in micelles, Colloid Surface A: Physicochemical Eng. Aspects 197, 7, (2002).
[12] R. Roy, A. 1990, Primer on the Taguchi Method, Van Nostrand Reinhold New York.
[13] P. Sharma, A. Verma, R.K. Sidhu, and O.P. Pandey, Process parameter selection for strontium ferrite sintered magnets using Taguchi L9 orthogonal design, Journal of Materials Processing Technology 168, 147–151, (2005).
[14] K.D. Kim, S.H. Kim, and H.T. Kim, Applying the Taguchi method to the optimization for the synthesis of TiO2 nanoparticles by hydrolysis of TEOT in micelles, Colloids and Surface A: Physcochem. Eng. Aspects 254, 99-105, (2005).
[15] B.L. Cuching, V.L. Kolesnichenko, and C.J. Oconnor, Advanced Material Reseach Institute, University New Orleans, p.p. 3893-3946, (2004).
[16] R. Xu, and W. Wei, Fe modified CuMnZrO2 catalysts for higher alcohols synthesis from syngas: Effect of calcination temperature Juornal of Molecular Catalysis A: Chemical 234, 75-83, (2005).
[17] S. K. Ghosh, Functional coatings by polymer microencapsulation, pp. 259-279, (2006).
[18] J. Liu, and J. Shi, Surface active structure of ultra-fine Cu/ZrO2 catalysts used for the CO2 + H2 to methanol reaction, Applied Catalysis A: General 218, 113-119, (2001).